[39]D. Stauffer, Phys. Rev. B **6**, 1839 (1972).
[40]J. F. Nagle, Phys. Rev. A **2**, 2124 (1970); J. F. Nagle and J. C. Bonner, J. Chem. Phys. **54**, 729 (1971); J. C. Bonner and J. F. Nagle, J. Appl. Phys. **42**, 1280 (1971); W. K. Theumann and J. S. Hoye, J. Chem. Phys. **55**, 4159 (1971); J. S. Hoye, Phys. Rev. B **6**, 4261 (1972); A. Hankey, T. S. Chang, and H. E. Stanley, AIP Conf. Proc. **10**, 889 (1973).
[41]M. Wortis, D. Jasnow, and M. A. Moore, Phys. Rev. **185**, 805 (1969). See also the review article by M. Wortis, in *Phase Transitions and Critical Phenomena*, edited by C. Domb and M. S. Green (Academic, London, to be published), Vol. 3.
[42]F. Englert, Phys. Rev. **129**, 567 (1963).
[43]Thus, in vertex renormalization, one eliminates all so-called "one-insertions" from each skeletal vertex at the expense of replacing bare semi-invariants with renormalized semi-invariants. In bond renormalization, one replaces all "two-insertions" by a single bond which now no longer represents a simple exchange factor J but is rather a more complex correlation factor.
[44]For a study of correlation functions in finite field see D. Gaunt and G. A. Baker, Jr., Phys. Rev. B **1**, 1184 (1971).
[45]F. Harbus and H. E. Stanley, Phys. Rev. Lett. **29**, 58 (1972); the meta model has been recently studied for the special case $H=0$ by A. J. Guttmann, J. Phys. C **5**, 2460 (1972).
[46]M. A. Moore, D. Jasnow, and M. Wortis, Phys. Rev. Lett. **22**, 940 (1969).
[47]See the reviews of Ref. 6 for a general discussion of series-analysis methods; and also D. L. Hunter and G. A. Baker, Phys. Rev. B **7**, 3346 (1973) for a more detailed treatment and critique.
[48]Suppose the series for these models in both finite direct field H and staggered field H_{st} were somehow available. We note that it would be much more difficult to locate by series the critical lines terminating the wings. In the full three-dimensional H-T-H_{st} field space, a ray through the origin at some inclination to the H-T plane is not guaranteed to intersect the wing critical lines, though perhaps such series might be able to respond to singularities on the wings simply by coming close by.
[49]This problem and a bilinear transformation method to deal with it are discussed in M. H. Lee and H. E. Stanley, Phys. Rev. B **4**, 1613 (1971). See also Ref. 51.
[50]M. E. Fisher, Philos. Mag. **7**, 1731 (1962); M. F. Sykes and M. E. Fisher, Physica (Utr.) **28**, 919 (1962); Physica (Utr.) **28**, 939 (1962); M. E. Fisher, *Lectures in Theoretical Physics* (University of Colorado Press, Boulder, Colo., 1965), Vol. VIIc, pp. 1–159.
[51]D. D. Betts, C. J. Elliott and R. V. Ditzian, Can. J. Phys. **49**, 1327 (1971).
[52]We thank Professor R. B. Griffiths for very helpful discussions on this point; see also Ref. 12.

PHYSICAL REVIEW B VOLUME 8, NUMBER 3 1 AUGUST 1973

High-Temperature-Series Study of Models Displaying Tricritical Behavior. II. A Nearest-Neighbor Ising Antiferromagnet with Next-Nearest-Neighbor Ferromagnetic Interactions*

Fredric Harbus† and H. Eugene Stanley
Physics Department, Massachusetts Institute of Technology, Cambridge, Massachusetts 02139
(Received 16 February 1973)

The nnn model is an Ising model with nearest-neighbor antiferromagnetic interactions ($J_1 < 0$) but also next-nearest-neighbor ferromagnetic exchange ($J_2 > 0$). This model is analyzed in external magnetic field using the same techniques as applied to the meta model of Paper I. Again, the staggered susceptibility χ_{st} appears to diverge along the critical line in the H-T plane with a constant exponent $\gamma_{st} = 5/4$, consistent with the universality hypothesis. However, in contrast to the meta model, it is found that the direct susceptibility χ diverges at the tricritical point with an exponent $\bar{\gamma} \simeq 1/4$. Implications of the scaling hypothesis at the tricritical point are discussed and the results for both the meta and nnn models are utilized to obtain the scaling power $\tilde{a}_2$ corresponding to the "weak" direction (in the sense of Griffiths and Wheeler). Included in this discussion is the double-power-law form, predicted to hold within the crossover region by tricritical-point scaling.

I. INTRODUCTION

A next-nearest-neighbor (nnn) spin-$\frac{1}{2}$ Ising model with tricritical behavior was introduced in Eq. (2.4) of the preceding paper[1] (Paper I). The Hamiltonian is

$$\mathcal{H} = -J_1 \sum_{\langle ij \rangle}^{\text{nn}} s_i s_j - J_2 \sum_{[ij]}^{\text{nnn}} s_i s_j - \mu H \sum_i s_i \ . \qquad (1.1)$$

Here $J_1 < 0$ (antiferromagnetic), $J_2 > 0$ (ferromagnetic), and the first and second sums are over nearest-neighbor (nn) and nnn spins, respectively. H is a direct external field, and μ is the magnetic moment per site. The Hamiltonian is considered on the simple-cubic lattice.

We apply the same series-expansion techniques to this model (with $J_1 = -1$, and $J_2 = +\frac{1}{2}$) as were applied to the meta model of Paper I. We therefore do not repeat the discussion of the method of obtaining the series and of the various methods of analysis, but rather go directly to the results. The coefficients of the reduced-susceptibility and stag-

TABLE I. Coefficients a_n and b_n through order $n=8$ in the series for the reduced susceptibility $\bar{\chi}=\sum_{n=0}^{\infty} a_n \beta^n$ and staggered susceptibility $\bar{\chi}_{st}=\sum_{n=0}^{\infty} b_n \beta^n$, respectively. Here $\beta \equiv 1/k_B T$, and the expansion variable X denotes $\tanh^2 h \equiv \tanh^2(\mu H/k_B T)$. When computer roundoff made it impossible to determine the exact fractions for the $n=7,8$ coefficients, the numbers quoted there are to be regarded as uncertain in the last digit.

	$b_0 = 1 - X$
$a_0 = 1 - X$	$b_1 = 12 - 24X + 12X^2$
$a_1 = 0$	$b_2 = 135 - 393X + 381X^2 - 123X^3$
$a_2 = -9 + 63X - 99X^2 + 45X^3$	$b_3 = 1475 - 5548X + 7802X^2 - 4860X^3 + 1131X^4$
$a_3 = -45 + 468X - 1158X^2 + 1092X^3 - 357X^4$	$b_4 = 15\,848\tfrac{1}{4} - 72\,626\tfrac{3}{4}X + 132\,506\tfrac{1}{2}X^2 - 120\,237\tfrac{1}{2}X^3 + 54\,221\tfrac{1}{4}X^4 - 9711\tfrac{3}{4}X^5$
$a_4 = -207\tfrac{3}{4} + 2309\tfrac{1}{4}X - 6421\tfrac{1}{2}X^2 + 7522\tfrac{1}{2}X^3 - 3978\tfrac{3}{4}X^4 + 776\tfrac{1}{4}X^5$	
$a_5 = -1163\tfrac{1}{4} + 12\,447X - 28\,181\tfrac{1}{4}X^2 + 11\,364X^3 + 27\,950\tfrac{1}{4}X^4 - 32\,523X^5 + 10\,106\tfrac{1}{4}X^6$	$b_5 = 168\,488\tfrac{7}{20} - 908\,292\tfrac{1}{5}X + 2\,029\,310\tfrac{7}{20} - 2\,403\,660X^3 + 1\,590\,716\tfrac{1}{4}X^4 - 557\,163X^5 + 80\,600\tfrac{1}{4}X^6$
$a_6 = -7901\tfrac{2}{5} + 95\,028\tfrac{3}{10}X - 232\,453\tfrac{9}{10}X^2 + 30\,821X^3 + 578\,546X^4 - 855\,502\tfrac{1}{2}X^5 + 499\,492\tfrac{1}{2}X^6 - 108\,030X^7$	$b_6 = 1\,778\,367 - 11\,012\,351\tfrac{29}{30}X + 29\,071\,209\tfrac{13}{20}X^2 - 42\,391\,526\tfrac{7}{15}X^3 + 36\,858\,716X^4 - 19\,099\,510\tfrac{1}{2}X^5 + 5\,458\,474\tfrac{1}{2}X^6 - 663\,378X^7$
$a_7 = -59\,260\tfrac{1}{8} + 865\,472\tfrac{7}{10}X - 3\,004\,164\tfrac{7}{10}X^2 + 3\,862\,762\tfrac{3}{10}X^3 - 368\,327.556X^4 - 4\,044\,663.475X^5 + 4\,263\,150.442X^6 - 1\,792\,051.429X^7 + 277\,081.839X^8$	$b_7 = 18\,672\,528.8 - 130\,520\,263.6X + 397\,184\,660.3X^2 - 687\,109\,994.5X^3 + 738\,943\,655.6X^4 - 505\,820\,047.5X^5 + 215\,222\,978.5X^6 - 52\,056\,811.5X^7 + 5\,483\,293.9X^8$
$a_8 = -467\,270.90 + 8\,077\,350.43X - 36\,155\,052.39X^2 + 77\,956\,034.52X^3 - 101\,070\,262.40X^4 + 94\,944\,384.31X^5 - 75\,848\,467.57X^6 + 49\,153\,249.20X^7 - 20\,251\,527.13X^8 + 3\,661\,562.07X^9$	$b_8 = 195\,283\,040 - 1\,520\,235\,353.X + 5\,236\,421\,559.X^2 - 10\,473\,683\,887.X^3 + 13\,406\,060\,143.X^4 - 11\,388\,951\,289.X^5 + 6\,423\,531\,645.X^6 - 2\,320\,682\,643.X^7 + 487\,762\,686.X^8 - 45\,505\,905.X^9$

gered-susceptibility series are presented in Table I; these series are analyzed in subsequent sections.

It is to be stressed at the outset that over-all series convergence was *better* for the nnn model than for the meta model. This is not unexpected, since with nnn bonds the lattice is effectively more closely packed than with nearest-neighbor bonds only, in the sense that a given number of high-temperature-series terms are better able to "feel out" critical behavior. On the other hand, the fact that these models incorporate bonds of opposite sign, giving rise to cancellations in the graphical expansion, makes predictions concerning relative convergence more difficult to make in advance.

At the end of this paper, we discuss the results for both the meta and nnn models in the light of a scaling hypothesis at the tricritical point (TCP). The estimates for the direct tricritical susceptibility exponents $\bar{\gamma}$ are used to obtain values for the tricritical scaling power corresponding to the "weak" direction in the sense of Griffiths and Wheeler.[2] Other tricritical scaling powers unfortunately cannot be obtained with any reasonable accuracy. We pay particular attention to the double-power-law form predicted by TCP scaling to hold within the crossover region bounding the critical line near the TCP. Several factors, most notably the differing values for $\bar{\gamma}$, cause us to conclude that the two tricritical models show significant differences in critical behavior, despite the fact that they are both three-dimensional Ising models.

II. CRITICAL-LINE ANALYSIS

A. Ratio Method

The plots of the ratios $\rho_l(h)$ vs $1/l$ for the nnn $\bar{\chi}_{st}$ series along paths of $h \equiv \mu H/k_B T$ ranging from 0 to 0.6 are shown in Fig. 1. These series do not exhibit the oscillations observed in ratio plots for the $\bar{\chi}_{st}$ series of the meta model, and *estimates from them may be made directly without the necessity of a bilinear transformation*. Examination of the ratio plots reveals a slight downward curvature, which is more pronounced at higher h. To have our analysis take account of this curvature, we use both a slightly modified version of the ratio method and also Neville-table analysis. The estimates from these methods, along with the eighth-order Padé-approximant analysis of Sec. II B, were all mutually consistent and hence lent confidence to the correctness of the critical temperatures which were determined.

First, we define the sequence of estimates $k_B T_c^{(l)}(h)$ by

$$k_B T_c^{(l)}(h) = l\rho_l(h) - (l-1)\rho_{l-1}(h) \ . \qquad (2.1)$$

We then consider the sequence of linear extrapolants of this sequence, where the lth *extrapolated* critical point is given by

$$T_c^{(l)\,\mathrm{ex}}(h) = lT_c^{(l)}(h) - (l-1)T_c^{(l-1)}(h) \ . \qquad (2.2)$$

This extrapolation procedure was complemented by calculation of complete Neville-table sequences for the critical temperature at various fields. In this method the mth-order set of extrapolants $\{t_l^{(m)}\}$ is defined by

$$t_l^{(m)} = [lt_l^{(m-1)} - (l-m)t_{l-1}^{(m-1)}]/m \ , \qquad (2.3)$$

where $t_l^{(0)} \equiv \rho_l$, the original ratios. We show in Table II Neville sequences for fields from $h = 0.0$–0.5. The $t_l^{(1)}$ entries coincide with the sequence determined from Eq. (2.1). The critical temperatures from Table II are estimated to be $k_B T_c(0.0) = 10.15 \pm 0.01$, $k_B T_c(0.1) = 10.07 \pm 0.02$, $k_B T_c(0.2) = 9.85 \pm 0.02$, $k_B T_c(0.3) = 9.48 \pm 0.02$, $k_B T_c(0.4) = 9.00 \pm 0.03$, and $k_B T_c(0.5) = 8.46 \pm 0.04$.

The Neville-table estimates are all quite consistent with the final estimate of Eq. (2.2), the $T_c^{(8)\,\mathrm{ex}}$. The latter seemed reasonable choices for best estimates of the critical temperatures. The sequence of exponents $\gamma_{st}^{(l,8)}$ is then calculated according to

$$\gamma_{st}^{(l,8)} = 1 - l[1 - \rho_l(h)/k_B T_c^{(8)\,\mathrm{ex}}(h)] \ . \qquad (2.4)$$

Finally, from the set $\{\gamma_{st}^{(l,8)}\}$, we form the set of *extrapolated* exponents $\{\gamma_{st}^{(l,8)\,\mathrm{ex}}\}$ defined by

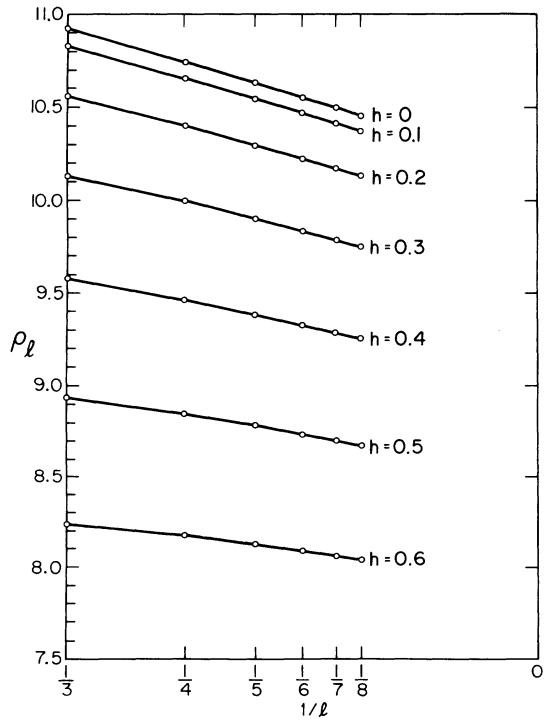

FIG. 1. Ratio plots ρ_l vs $1/l$ for staggered-susceptibility series $\bar{\chi}_{st}(h)$ at various values of $h \equiv \mu H/kT$ (cf. Fig. 4 of Paper I).

$$\gamma_{st}^{(l,s)\,ex} = l\gamma_{st}^{(l,s)} - (l-1)\gamma_{st}^{(l-1,s)} \quad . \tag{2.5}$$

In Fig. 2 we show in a $1/l$ plot the estimates for γ_{st} for the $h=0$ $\bar{\chi}_{st}$ series. The lower curve is the set $\{\gamma_{st}^{(l,s)}\}$, while the upper curve is the set $\{\gamma_{st}^{(l,s)\,ex}\}$. The latter set is seen to converge to the expected value of 1.25 slightly faster than the former. Figure 3 shows the extrapolated exponents for several nonzero field paths. We emphasize that although we have plotted the γ_{st} estimates on a very finely grained scale in Figs. 2 and 3 with three decimal places shown, the estimates are to be regarded as accurate to only two decimal places. With series of this length no real significance should be attached to the last decimal place; we have included three decimal places in the figures to convey somewhat more detailed information about the degree of convergence than would be possible if we rounded off to the nearest hundredth. Rounding off would reduce several of the different field plots

TABLE II. Neville-table estimates for critical temperatures for various h paths. The entry $t_l^{(m)}$ is given by Eq. (2.3) in the text.

l	$t_l^{(1)}$	$t_l^{(2)}$	$t_l^{(3)}$	$t_l^{(4)}$	$t_l^{(5)}$	$t_l^{(6)}$	$t_l^{(7)}$
				(a) $h=0$			
3	10.28	10.17					
4	10.20	10.12	10.11				
5	10.18	10.15	10.16	10.17			
6	10.17	10.16	10.17	10.18	10.18		
7	10.17	10.16	10.17	10.16	10.16	10.15	
8	10.17	10.16	10.16	10.15	10.14	10.14	10.14
				(b) $h=0.1$			
3	10.20	10.10					
4	10.13	10.05	10.03				
5	10.10	10.07	10.08	10.09			
6	10.09	10.08	10.09	10.10	10.10		
7	10.09	10.08	10.09	10.09	10.08	10.08	
8	10.09	10.08	10.08	10.07	10.07	10.06	10.06
				(c) $h=0.2$			
3	9.99	9.90					
4	9.91	9.83	9.81				
5	9.88	9.83	9.83	9.84			
6	9.87	9.85	9.86	9.87	9.88		
7	9.86	9.85	9.86	9.86	9.86	9.86	
8	9.86	9.85	9.85	9.85	9.83	9.83	9.82
				(d) $h=0.3$			
3	9.65	9.59					
4	9.57	9.48	9.44				
5	9.53	9.46	9.45	9.45			
6	9.51	9.48	9.49	9.51	9.52		
7	9.50	9.49	9.50	9.51	9.50	9.50	
8	9.50	9.49	9.49	9.48	9.47	9.46	9.45
				(e) $h=0.4$			
3	9.21	9.18					
4	9.12	9.03	8.98				
5	9.06	8.99	8.97	8.96			
6	9.04	9.00	9.02	9.05	9.07		
7	9.04	9.02	9.03	9.04	9.04	9.03	
8	9.03	9.02	9.02	9.01	8.99	8.97	8.97
				(f) $h=0.5$			
3	8.69	8.69					
4	8.59	8.48	8.42				
5	8.52	8.43	8.39	8.39			
6	8.50	8.46	8.48	8.52	8.55		
7	8.49	8.47	8.49	8.49	8.48	8.47	
8	8.49	8.47	8.47	8.45	8.42	8.41	8.40

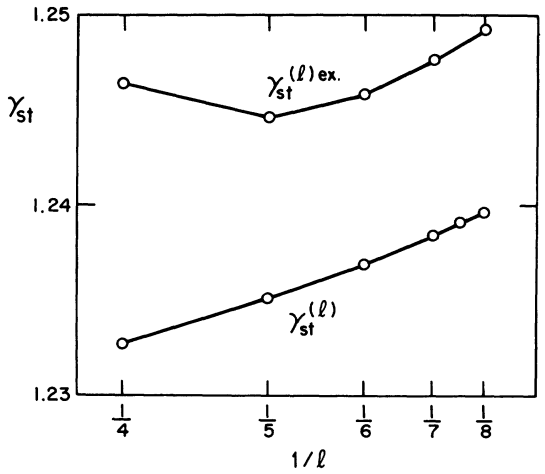

FIG. 2. Ratio-method estimates of exponent γ_{st} for zero field, $h=0$. The lower sequence is the set determined from Eq. (2.4), while the upper sequence is a set of linearly extrapolated exponents, calculated according to Eq. (2.5).

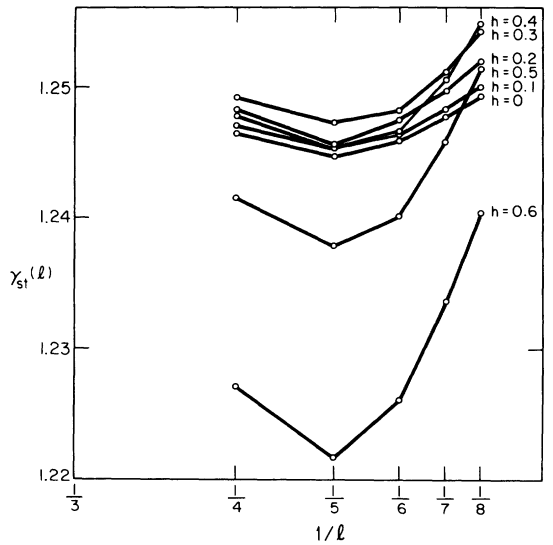

FIG. 3. Ratio-method estimates of exponent γ_{st} for several nonzero field paths as well as $h=0$. These are sequences of linearly extrapolated exponents. Note the fineness of the scale of the ordinate. The last decimal place in the estimates is not, however, to be regarded as significant.

TABLE III. Estimates of exponents γ_{st} and critical temperatures T_c for various $h \equiv \mu H/k_B T_c$ values. Here γ_{st}^R is the last linear extrapolant of the sequence of Eq. (2.5) in the text. The $k_B T_c^R$ are the $k_B T_c^{(8)ex}$ determined from Eq. (2.2). The last column shows the critical temperature obtained from PA's to $[\bar{\chi}_{st}(h)]^{4/5}$. Besides the extreme closeness of the γ_{st}^R to $\frac{5}{4}$, the excellent agreement between the two sets of T_c strongly supports the universality-hypothesis prediction along the second-order line.

h	γ_{st}^R	$k_B T_c^R$	$k_B T_c^P$
0	1.25	10.15	10.15
0.1	1.25	10.07	10.07
0.2	1.25	9.84	9.84
0.3	1.25	9.47	9.48
0.4	1.25	9.00	9.00
0.5	1.25	8.45	8.45
0.6	1.24	7.85	7.84
0.7	1.22	7.24	7.23
0.8	1.18	6.64	6.61

of Fig. 3 to a string of points right at 1.25, misleadingly implying some sort of perfect convergence.

The slight curvature on these scales is therefore not, we believe, a real effect pointing to values of γ_{st} higher than 1.25. Consider, for example, the behavior of the zero-field points of Fig. 3. For $h = 0$, the staggered susceptibility must diverge the same way as the direct susceptibility in the corresponding Ising ferromagnet, for which case the exponent is well established to be 1.25. Yet the zero-field points show some curvature which is mimicked by the finite-field plots. We think any systematic trend is also ruled against by the decrease of the estimates for the fields beyond $h = 0.4$.

As a final consistency check using ratios, we analyzed the series by fixing the exponent at $\frac{5}{4}$ and examining the sequence of T_c's then obtained. While the sequence of T_c's fell slightly lower than the $T_c^{(8)\,ex}$, they form an increasing sequence whose trend is to values at least as high as $T_c^{(8)\,ex}$. The estimates obtained in this method are consistent with the Neville-table estimates.

Table III summarizes some of the information obtained from ratio-plot analysis for several field paths. Only two significant decimal places have now been retained in the γ_{st}^R entries.

B. Padé Approximants

The same Padé-approximant (PA) operations were performed for the nnn model series as for the meta series, and we therefore present a relatively brief discussion here. The log-Padé results for $\bar{\chi}_{st}$ series along several different h paths are shown in Table IV, and Table V gives the PA's to these series raised to the $\frac{4}{5}$ power. Unlike the meta series, the log Padés here appear to converge reasonably well. The exponents they predict fall systematically lower than 1.25, however, and the critical temperatures are slightly greater than those predicted from the ratio method. The departure from 1.25 increases as the field increases, although even at $h = 0$ the exponent converges to only 1.23. In light of our estimates from the ratio method and the additional evidence from the PA to $(\bar{\chi}_{st})^{4/5}$ operation, we believe this decrease in exponent to be a spurious effect which would not occur were sufficiently longer series being analyzed.

It is interesting that a somewhat similar decrease of exponent is observed as the critical temperature decreases toward the tricritical temperature in Oitmaa's high-temperature series analysis[3] of the Blume-Emery-Griffiths lattice model for He^3-He^4 mixtures [Eq. (2.2) of I]. In that model, the direct susceptibility is the strongly divergent quantity along the critical line; the universality hypothesis predicts it diverges with a constant $\frac{5}{4}$ power. As in the models we have considered, the series become more irregular at values of the "field" Δ parametrizing the critical line which lie closer to the TCP, and the series analysis indicates singularities beyond the point estimated to be the TCP.

The last column in Table III gives the singularities $k_B T_c^P(h)$ estimated from PA's to $[\bar{\chi}_{st}(h)]^{4/5}$ along the various h paths. Agreement with $k_B T_c^R(h)$ is excellent up to $h \cong 0.7$, and even the $h = 0.8$ values differ by only 0.5%. As in the meta analysis, we notice that when $T_c^R(h) > T_c^P(h)$, the estimated exponent γ_{st}^R is less than 1.25. We believe the extreme proximity of γ_{st}^R to $\frac{5}{4}$, and the excellent agreement between the $T_c^R(h)$ and $T_c^P(h)$ provide strong support for the universality hypothesis prediction of a constant $\frac{5}{4}$ exponent for γ_{st} along the second-order line, at least for fields up to those corresponding to $h \cong 0.6$ ($\mu H_c \cong 4.7$).

We take the $T_c^P(h)$ estimates as the best values with which to map out the critical line in the H-T plane. As for the meta model, h is incremented up from 0 by steps of 0.02, and the set of phase-boundary points (T_c, H_c) shown in Fig. 4 is located. The $T = 0$ critical field is given by arguments similar to those applied to the meta model and we obtain

$$\mu H_c(0) = q_1 |J_1| \tag{2.6}$$

or $\mu H_c(0) = 6$ for the parameters $q_1 = 6$, $J_1 = -1$.

The calculated singularities hook downward for large h, and it is quite plausible that they represent the "spinodal" curve, i.e., the analytic continuation of the critical line into the ordered antiferromagnetic phase. Joining the calculated phase boundary to the $T = 0$ critical field value by a curve that meets the critical line with continuous slope locates the TCP in the region of $k_B T_c \cong 6.40$, or $h \cong 0.84$.

TABLE IV. Log-Padé tables for $\bar{\chi}_{st}$ series along various h paths. In parentheses below each pole is the corresponding residue. The notation ··· denotes the fact that no physical pole appeared in that entry of the table.

D \ N	1	2	3	4	5
			(a) $h=0$		
2	10.14 (1.25)	10.16 (1.24)	10.16 (1.23)	10.16 (1.23)	10.16 (1.23)
3	10.16 (1.24)	10.16 (1.23)	10.16 (1.23)	10.16 (1.23)	
4	10.16 (1.23)	10.16 (1.23)	10.16 (1.23)		
5	10.16 (1.23)	10.16 (1.23)			
6	10.16 (1.23)				
			(b) $h=0.2$		
2	9.82 (1.25)	9.85 (1.23)	9.85 (1.23)	9.85 (1.23)	9.85 (1.23)
3	9.85 (1.23)	9.86 (1.23)	9.85 (1.23)	9.85 (1.23)	
4	9.85 (1.23)	9.85 (1.23)	9.84 (1.24)		
5	9.85 (1.23)	9.85 (1.23)			
6	9.85 (1.24)				
			(c) $h=0.4$		
2	9.45 (1.14)	8.98 (1.25)	9.03 (1.21)	9.03 (1.21)	9.03 (1.21)
3	8.98 (1.25)	9.03 (1.20)	9.03 (1.21)	9.03 (1.21)	
4	9.03 (1.21)	9.03 (1.21)	9.02 (1.21)		
5	9.03 (1.21)	9.03 (1.21)			
6	9.03 (1.21)				
			(d) $h=0.6$		
2	8.08 (1.06)	7.82 (1.24)	7.89 (1.16)	7.89 (1.16)	7.88 (1.18)
3	7.79 (1.28)	7.91 (1.15)	7.89 (1.16)	7.90 (1.15)	
4	7.89 (1.16)	7.89 (1.16)	7.89 (1.17)		
5	7.89 (1.16)	7.89 (1.16)			
6	7.87 (1.19)				
			(e) $h=0.8$		
2	6.85 (0.97)	6.65 (1.11)	6.69 (1.07)	6.68 (1.08)	6.56 (1.92)
3	6.62 (1.15)	6.70 (1.06)	6.69 (1.07)	···	
4	6.69 (1.07)	6.69 (1.07)	6.67 (1.09)		
5	6.68 (1.07)	6.69 (1.07)			
6	6.70 (1.07)				

C. Mean-Field-Theory Predictions

Finally, we mention and compare with the mean-field-theory (MFT) predictions near the Néel point. The series value for the Néel temperature is $k_B T_N^{(ser)} = 10.15 < k_B T_N^{(MF)} = q_1|J_1| + q_2 J_2 = 6 + 12(\frac{1}{2}) = 12$. Despite the discrepancy in absolute critical temperatures, the shape of the phase boundary near T_N is again fairly well described by MFT, which predicts $(\mu H_c)^2 = 14.2 k_B(T_N - T_c)$. Figure 5 is a plot of $(\mu H_c)^2$ vs $k_B(T_N - T_c)$ for points near T_N, along with a few straight-line fits. The MF line is seen to be close to the calculated points at low fields.

III. TRICRITICAL-POINT ANALYSIS

In Sec. II, we estimated the tricritical point to occur for $h_t \cong 0.84$. Along this path, the susceptibility series is

$$\bar{\chi}(h=0.84) = 0.529\,666 + 3.41\,285\beta^2 + 15.0970\beta^3 + 63.6808\beta^4 + 367.884\beta^5 + 2056.62\beta^6 + 11\,709.0\beta^7 + 68\,793.0\beta^8 \ . \quad (3.1)$$

Although the coefficients are all positive and monotonically increasing (in contrast to the meta model), ratio methods still do not produce convergent enough results to be of significant value. However, the $\bar{\chi}$ series is evidently better behaved than for the meta case, and we will see shortly that the Padé methods do indeed produce rather well-convergent results.

Turning our attention momentarily to $\bar{\chi}_{st}$, we show in Table VI the PA to the series $[\bar{\chi}_{st}(h=0.84)]^{4/5}$. From this table we estimate a critical temperature of $k_B T_c = 6.37 \pm 0.02$. The log-Padé operation to $\bar{\chi}(0.84)$ yielded the table of singularities and residues shown in Table VII. Convergence, although not excellent, is far superior to the corresponding table for the meta model, Table VI of Paper I. Most of the singularities of Table VII are in the range $k_B T_c = 6.4 \pm 0.1$, in good agreement with the $\bar{\chi}_{st}$ singularity. Furthermore, one may see that the exponent $\bar{\gamma}_{nnn}$ lies in the range $\bar{\gamma}_{nnn} \sim 0.2 - 0.3$, with

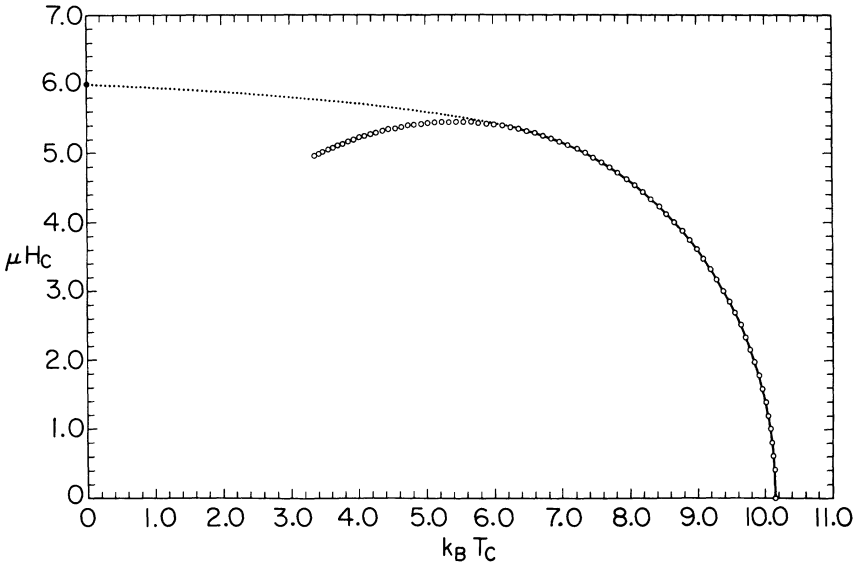

FIG. 4. Phase boundary for nnn model with $J_1 = -1$, $J_2 = +\frac{1}{2}$. The second-order portion of the phase line is shown solid, and the first-order portion dotted. The series analysis indicates singularities below $k_B T_c \cong 6.4$, which hook downward into the antiferromagnetic phase.

a value about 0.25 for critical temperatures closest to $k_B T_c = 6.4$. To pin down the exponent and tricritical temperature more precisely, we carry out the procedure of raising the $\overline{\chi}$ series along various paths near $h = 0.84$, including $\overline{\chi}(h = 0.84)$ itself, to a variety of powers equal to and near the inverse of 0.25.

A sample of the results is presented in Tables VIII–X. Since the interpretation of the data follows similar lines as for the meta model of Paper I, we give only a brief discussion. Shown in parts (a)–(c) of Table VIII are Padé tables for the $\overline{\chi}(0.84)$ series raised to the inverse of 0.2, 0.25, and 0.30 respectively. It is evident that convergence of the $\overline{\chi}^4$ Padé [part (b)] is the best; moreover, it converges to a critical temperature in excellent agreement with that from Table VI. This is also the case along $h = 0.82$ and $h = 0.86$. Convergence and consistency with the $\overline{\chi}_{st}$ root are best for $\overline{\chi}^4$. However, the agreement between the $\overline{\chi}$ and $\overline{\chi}_{st}$ roots is not quite as close as for $h = 0.84$.

The next two tables display the Padés to $\overline{\chi}$ raised to the same set of powers as in Table VIII, but along paths slightly further away from $h = 0.84$. Tables IX and X are for $h = 0.80$ and 0.88, respectively, for which the $\overline{\chi}_{st}$ analysis locates singularities at $k_B T_c \cong 6.61$ and 6.13. Convergence for the $\overline{\chi}^4$ Padé is now not nearly as good as for $h = 0.84$, nor is the $\overline{\chi}^4$ Padé clearly the best convergent of the three powers shown. However, neither the $\overline{\chi}^5$ nor $\chi^{10/3}$ Padés along either path reproduce the corresponding $\overline{\chi}_{st}$ critical temperature with the accuracy of $\overline{\chi}^4$ in the $h = 0.82$–0.86 range.

We conclude that for this model, $h_t \cong 0.84 \pm 0.02$, corresponding to $T_t/T_N = 0.63 \pm 0.01$. As in the meta model, the location of the TCP was independently confirmed by Monte Carlo methods.[4]

The susceptibility at the tricritical point behaves as

$$\overline{\chi}_{nnn} \sim (T - T_t)^{-1/4}, \tag{3.2}$$

with an uncertainty in the exponent $\overline{\gamma}_{nnn}$ of at most 0.05. We are able to be somewhat more confident about the error bars here than in the meta model. The value for $\overline{\gamma}$ obtained[5] by Monte Carlo techniques

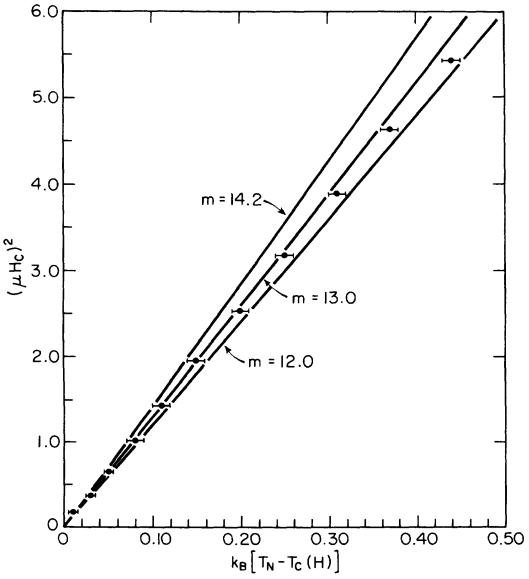

FIG. 5. Plot of $(\mu H_c)^2$ vs $k_B[T_c(H) - T_N]$. Lines of three different slopes are drawn for comparison. The mean-field-theory prediction is $m = 14.2$, which is clearly not the best fit at higher fields ($\mu H_c \gtrsim 1$). For very small fields, where we expect the square law to hold best, it is impossible to distinguish the three lines (cf. Fig. 8 of Paper I).

TABLE V. Singularities given by PA table to $(\bar{\chi}_{st})^{4/5}$ for various h paths.

D \ N	1	2	3	4	5	6
			(a) $h=0$			
2	10.13	10.13	10.14	10.15	10.15	10.15
3	10.13	10.15	10.15	10.15	10.15	
4	10.14	10.15	10.15	10.15		
5	10.15	10.15	10.15			
6	10.15	10.15				
7	10.15					
			(b) $h=0.2$			
2	9.80	9.82	9.83	9.83	9.84	9.84
3	9.82	9.83	9.84	9.84	9.84	
4	9.83	9.84	9.84	9.84		
5	9.83	9.84	9.84			
6	9.84	9.84				
7	9.84					
			(c) $h=0.4$			
2	8.95	8.97	8.98	8.98	8.99	9.00
3	8.97	8.98	9.12	9.00	9.00	
4	8.98	9.10	9.01	9.00		
5	8.98	9.00	9.00			
6	8.99	9.00				
7	9.00					
			(d) $h=0.6$			
2	7.79	7.79	7.80	7.82	7.84	7.84
3	7.79	7.79	7.57	7.84	7.84	
4	7.80	7.56	7.82	7.84		
5	7.82	7.84	7.84			
6	7.83	7.84				
7	7.84					
			(e) $h=0.8$			
2	6.53	6.50	6.54	6.59	6.61	6.61
3	6.50	6.52	6.71	6.61	6.61	
4	6.54	6.68	6.60	6.61		
5	6.57	6.60	6.61			
6	6.59	6.61				
7	6.60					

on the same model with different parameters ($J_2/J_1 = -\frac{1}{4}$ instead of $-\frac{1}{2}$), was $\bar{\gamma}_{nnn} = 0.29 \pm 0.18$, which is within the error bars of our series result.

Comparison with Mean-Field Theory

The ratio T_t/T_N is predicted by MFT to be

$$\left(\frac{T_t}{T_N}\right)^{MF} = 1 - \frac{q_1|J_1|}{3q_2J_2} = \frac{2}{3} \tag{3.3}$$

for $J_1 = -1$, $J_2 = \frac{1}{2}$, $q_1 = 6$, $q_2 = 12$. Thus MFT evidently does somewhat better in estimating this ratio for the nnn model than the meta model. Again the MF prediction is greater, but only slightly, than the series result. However, a look at the Monte Carlo results[5] in the nnn model shows that it is wrong to generalize that MFT will always overestimate this ratio. In the Monte Carlo study, calculations were done on the two-dimensional square lattice with $J_2/J_1 = -\frac{1}{2}$, and on the simple-cubic lattice with $J_2/J_1 = -\frac{1}{4}$. For both cases MFT predicts that $T_t/T_N = \frac{1}{3}$. The data, however, indicate that $T_t/T_N \cong 0.35$ on the square and $\cong 0.42$ on the sc lattices, values greater than $\frac{1}{3}$. Hence no regular trend in the behavior of the MFT prediction for T_t/T_N is easily recognizable. Finally, we mention again that MFT predicts *no* divergence in $\bar{\chi}$ at T_t as the TCP is approached from above, while our numerical evidence suggests that a law of the form of Eq. (3.2) is obeyed.

TABLE VI. Singularities given by PA's to the series $[\bar{\chi}_{st}(h=0.84)]^{4/5}$. The critical temperature is estimated to be $k_BT_c = 6.37 \pm 0.02$.

D \ N	2	3	4	5	6
2	6.25	6.29	6.35	6.36	6.37
3	6.27	6.45	6.36	6.37	
4	6.43	6.35	6.37		
5	6.36	6.37			
6	6.37				

IV. TRICRITICAL-POINT SCALING

Riedel developed[6] a scaling theory for TCP's in close analogy with parameter-scaling theories earlier applied to anisotropic magnetic systems.[7] He formulates a "principle of competition" in the TCP region between TCP-dominated critical behavior and critical line-dominated behavior. This competition leads to crossover and "double-power law" effects which may be predicted in terms of the scaling powers and fields.

We find it most convenient in our discussion to adopt the generalized homogeneous function (GHF) approach to TCP's of Hankey *et al.*[8], who extended Riedel's work to the full three-dimensional field space of Fig. 1(c) of Paper I). It is crucial to choose

TABLE VII. Singularities given by log-Padé method to $\bar{\chi}(h=0.84)$ series. Beneath each pole is the corresponding residue. The notation ··· denotes the fact that no physical pole appeared in that entry.

D \ N	1	2	3	4	5
2	···	5.50 (0.47)	6.56 (0.21)	6.49 (0.22)	6.48 (0.23)
3	6.51 (0.24)	6.15 (0.30)	6.43 (0.24)	6.48 (0.23)	
4	6.01 (0.34)	6.28 (0.27)	6.53 (0.21)		
5	6.46 (0.23)	6.41 (0.24)			
6	6.40 (0.25)				

TABLE VIII. Singularities given by PA's to $[\bar{\chi}(h=0.84)]^p$, with (a) $p=5$, (b) $p=4$, and (c) $p=\frac{10}{3}$. It is clear that convergence is best for the series $\bar{\chi}^4$, part (b), from which the critical temperature is estimated to be 6.39 ± 0.01. This is in excellent agreement with the value of T_c obtained from the $\bar{\chi}_{st}$ analysis along this path (cf. Table V).

D \ N	2	3	4	5	6
		(a) $p=5$			
2	6.32	7.03	7.15	6.57	6.61
3	6.73	6.69	6.63	6.60	
4	6.68	6.85	6.58		
5	6.60	6.54			
6	6.57				
		(b) $p=4$			
2	5.91	6.89	6.57	6.35	6.42
3	6.37	6.39	6.38	6.39	
4	6.39	6.38	6.39		
5	6.38	6.39			
6	6.39				
		(c) $p=\frac{10}{3}$			
2	5.60	7.00	6.31	6.19	6.32
3	6.10	6.18	6.21	6.24	
4	6.15	6.24	5.98		
5	6.17	6.52			
6	6.20				

the scaling fields at the TCP correctly.[9] In particular, the only direction at the TCP which is singled out is one parallel to the phase boundary there, and this is taken to be the $\bar{x}_3$ direction. The other two scaling directions consist of any vector pointing out of the coexistence surface (CXS), the "strong" direction $\bar{x}_1$ of Ref. 2, and one in the plane of the CXS but not parallel to the critical line at the TCP, the "weak" direction $\bar{x}_2$. Specializing to our antiferromagnetic models, we take $\bar{x}_1$ to be H_{st}, and $\bar{x}_2$ orthogonal to $\bar{x}_3$ in the H-T plane, so that the three scaling fields $(\bar{x}_1, \bar{x}_2, \bar{x}_3)$ at the TCP are all mutually "orthogonal."[10] Then the scaling hypothesis at the TCP may be stated by assuming that the singular part of the Gibbs potential obeys the following GHF equation:

$$G(\lambda^{\bar{a}_1}\bar{x}_1,\ \lambda^{\bar{a}_2}\bar{x}_2,\ \lambda^{\bar{a}_3}\bar{x}_3) = \lambda G(\bar{x}_1, \bar{x}_2, \bar{x}_3)\ . \qquad (4.1)$$

Here $\lambda > 0$, the $\bar{a}_i$ are tricritical scaling powers, and Eq. (4.1) is taken to hold for small values of the arguments. This equation in turn determines all TCP exponents, the equation of the critical line in the plane, L_1, as $x_{2(c)} \sim x_{3(c)}^{\bar{a}_2/\bar{a}_3}$, and the equation of the crossover curve. The latter is also described by $x_{2(x)} \sim x_{3(x)}^{\bar{a}_2/\bar{a}_3}$, or $x_{2(x)} \sim x_{3(x)}^{1/\varphi}$, where $\varphi \equiv \bar{a}_3/\bar{a}_2$ is the crossover exponent. These equations, the formulas for the TCP exponents obtained by appropriate differentiation of Eq. (4.1), and the scaling "laws" relating them are described in detail elsewhere.[6,8,11]

The direct susceptibility exponent $\bar{\gamma}$ is given by

$$\bar{\gamma} = -(1 - 2\bar{a}_2)/\bar{a}_2\ , \qquad (4.2)$$

provided the TCP is approached along a path not asymptotically parallel to the critical line L_1. A constant H or T path, or the $H/T = \text{const}$ path used in our calculations, falls in this category.[12] On the other hand a constant magnetization path $M = M_t$ would pick up a different exponent since such a path

TABLE IX. Singularities given by PA's to $[\bar{\chi}(h=0.80)]^p$, with same powers p in parts (a), (b), and (c) as in Table VII.

D \ N	2	3	4	5	6
		(a) $p=5$			
2	6.31	7.40	6.97	6.71	6.77
3	6.81	6.79	6.76	6.75	
4	6.79	6.81	6.74		
5	6.76	6.73			
6	6.74				
		(b) $p=4$			
2	5.90	7.73	6.64	6.50	6.63
3	6.45	6.51	6.52	6.54	
4	6.49	6.54	6.46		
5	6.51	6.26			
6	6.53				
		(c) $p=\frac{10}{3}$			
2	5.59	9.14	6.43	6.35	6.61
3	6.19	6.31	6.37	6.39	
4	6.25	6.44	6.72		
5	6.25	6.62			
6	6.29				

TABLE X. Singularities given by PA's to $[\bar{\chi}(h=0.88)]^p$, with same powers p in parts (a), (b), and (c) as in Table VII.

D \ N	2	3	4	5	6
		(a) $p=5$			
2	6.29	6.84	...	6.43	6.45
3	6.64	6.59	6.49	6.45	
4	6.56	...	6.41		
5	6.43	6.35			
6	6.39				
		(b) $p=4$			
2	5.88	6.57	6.71	6.20	6.25
3	6.27	6.27	6.23	6.23	
4	6.27	6.27	6.23		
5	6.23	6.23			
6	6.23				
		(c) $p=\frac{10}{3}$			
2	5.57	6.46	6.23	6.03	6.12
3	6.00	6.05	6.06	6.08	
4	6.04	6.06	6.03		
5	6.05	5.96			
6	6.07				

is expected to come in parallel to L_1. One would observe an exponent renormalized by φ to give $\bar{\gamma}_{m=m_t} = \bar{\gamma}/\varphi = -(1-2\bar{a}_2)/\bar{a}_3$. Our values for $\bar{\gamma}_{\text{meta}}$ and $\bar{\gamma}_{\text{nnn}}$, obtained at constant $h \equiv \mu H/k_B T$ paths, imply that, if scaling holds,

$$\bar{a}_{2\,(\text{meta})} \cong \tfrac{2}{3}\,, \tag{4.3}$$

$$\bar{a}_{2\,(\text{nnn})} \cong \tfrac{4}{7}\,. \tag{4.4}$$

A second scaling hypothesis with different scaling powers appropriate to the critical line L_1 may be made. When combined with the TCP scaling hypothesis, a "double-power" law for thermodynamic functions results inside the crossover region where both laws are simultaneously assumed valid. Quantities here possess singular amplitudes characterized by a mixed exponent containing both TCP and critical-line scaling powers. For example, the staggered susceptibility is predicted[13] to vary as

$$\bar{\chi}_{\text{st}} \sim \bar{x}_3^{(\gamma_{st}-\bar{\gamma}_{st})/\varphi}\,(\bar{x}_2 + k\bar{x}_3^{1/\varphi})^{-\gamma_{\text{st}}}\,. \tag{4.5}$$

Here γ_{st} is the critical-line exponent of $\frac{5}{4}$, $\bar{\gamma}_{\text{st}}$ is an unknown TCP critical exponent defined on a path of approach not parallel to $L_1[\bar{\gamma}_{\text{st}} = -(1-2\bar{a}_1)/\bar{a}_2]$, and k describes the critical line $x_{2(c)} = -kx_{3(c)}^{1/\varphi}$. The second factor $(\bar{x}_2 + k\bar{x}_3^{1/\varphi})$ in Eq. (4.4) measures the distance of a point $(\bar{x}_2, \bar{x}_3)$ from the critical line, and corresponds to $[T - T_c(H)]$ in $\bar{\chi}_{\text{st}} \sim A(T_c)[T - T_c(H)]^{-\gamma_{\text{st}}}$, where now the amplitude $A(T_c)$ is shown explicitly. The divergence with a power of $\gamma_{\text{st}} = \frac{5}{4}$ expresses the smoothness-postulate prediction that close enough to L one will see ordinary critical-line exponents. The amplitude function $\bar{x}_3^{(\gamma_{\text{st}}-\bar{\gamma}_{\text{st}})/\varphi}$ corresponds to $A(T_c)$, and clearly contains information about $\bar{\gamma}_{\text{st}}$. If $\bar{a}_2$ and $\bar{a}_3$ are known, then $\bar{\gamma}_{\text{st}}$ could be used to determine $\bar{a}_1$. Thus in principle all *three* scaling powers $\bar{a}_i$ could be obtained from a knowledge of the in-plane $(H-T)$ amplitude behavior of $\bar{\chi}_{\text{st}}$, the shape of the phase boundary at the TCP to give $\varphi \equiv \bar{a}_3/\bar{a}_2$, and a value for $\bar{\gamma}$ which yields by itself the value for $\bar{a}_2$.

Despite this prescription's simplicity in principle, unfortunately in practice it cannot be carried out because of the numerical difficulties and uncertainties present in the TCP models. We believe the location of the TCP in these models is not precise enough to afford a reliable estimate of φ from the curvature of the phase boundary, nor is the phase boundary itself accurate enough near the TCP for a sensitive measurement. Even if the TCP were known more precisely, to calculate φ entails imposing a set of tangential and normal coordinates on the phase boundary at this point, a process which is subject to appreciable error.

The amplitude behavior of the function $\bar{\chi}_{\text{st}}$ may be ascertained from the Padé tables to $(\bar{\chi}_{\text{st}})^{1/\gamma_{\text{st}}} = (\bar{\chi}_{\text{st}})^{4/5}$. It would be desirable if the amplitudes were observed to fall sharply to zero at a certain value of external field, for then this could be used to help identify and pin down the TCP. For the meta model, however, it was observed that while the amplitudes decrease as the phase boundary is followed up to higher fields, they do not fall strictly to zero. The amplitudes continue decreasing beyond $h \cong 0.7$ in the region where the hook occurs. Thus it is impossible to provide a value for $\bar{\gamma}_{\text{st}}$ from this data; we feel, though, it can safely be claimed that $\bar{\gamma}_{\text{st (meta)}} < \gamma_{\text{st}}$ because of the general decreasing trend in the amplitudes. For the nnn model, the $\bar{\chi}_{\text{st}}$ amplitudes behaved quite differently, remaining quite constant along the phase boundary, up to and beyond the TCP. This behavior would suggest that $\bar{\gamma}_{\text{st (nnn)}} \cong \gamma_{\text{st}}$.

Double-power laws of the form of Eq. (4.5) are not entirely abstract, for they have been[14] verified numerically using series expansions for another problem where there is crossover between two universality classes. This latter work is for an Ising model with fixed in-plane interactions J and weak between-plane bonds RJ $(R > 0)$ in zero external field. As $R \to 0$, the lattice crosses over from three- to two-dimensional behavior. The special symmetry point analogous to the TCP is the point $R = 0$ in the three-dimensional "field" space of T, H, and R. We note that this problem has numerous significant advantages over the TCP models from a calculational point of view. The special point where a changeover of exponents occurs is known precisely, and the scaling directions are the same as the physical axes in the field space, i.e., R and $[T - T_c(R=0)]$. Of course, the two-dimensional Ising exponents are either known exactly or known very well from series, and even the crossover exponent for this model has been rigorously determined.[15] Thus double-power laws here are not of practical use in actually finding unknown exponents. Nonetheless, this model illustrates the validity of double-power laws in at least one instance, and provides several tests of our methods and programs. It shows how double-power laws have the potential to be quite powerful in situations where exponents are not all known in advance.

We conclude this section with a brief survey of the status of TCP scaling in the three TCP models where series or Monte Carlo work has been done—the meta model, the nnn model, and the BEG model. The Monte Carlo work[5,16] has been able to supply estimates for the tricritical exponent $\bar{\beta}$ for the meta and nnn models: $\bar{\beta}_{\text{meta}} = 0.5 \pm 0.1$ and $\bar{\beta}_{\text{nnn}} = 0.78 \pm 0.2$, respectively. Scaling theory predicts $\bar{\beta} = (1-\bar{a}_2)/\bar{a}_3$, so these values coupled with the $\bar{a}_2$ of Eqs. (4.3) and (4.4) may be used to obtain $\bar{a}_3$. The result is that $\bar{a}_3 \cong \bar{a}_2$ for each model, which consequently predicts $\varphi \cong 1$ and a nearly linear phase boundary at the TCP. While such behavior is not impossible, it seems highly unlikely. Our

estimates of the curvature of L_1 near the TCP, which for the reasons explained above must be regarded as very rough, give $\varphi \approx \frac{1}{2}$ for the meta model, and $\varphi \approx 0.5 - 0.7$ for the nnn model. One could of course not rule out a change in curvature very close in to the TCP.

In the BEG model, the series data of Ref. 17 is fit by a sum of singular terms rather than the product form of Eq. (4.5). Assuming that the term whose amplitude is finite at the TCP furnishes an estimate for the TCP exponent, it may be shown that the scaling-predicted value for the amplitude which vanishes at the TCP is consistent within the error bars with the quoted values for φ and the power describing the vanishing amplitude.[17] More recent calculations on this model by the same group, however, indicate a possible violation of tricritical scaling.[18]

V. CONCLUSIONS

In this work we have obtained high-temperature series expansions for two spin-$\frac{1}{2}$ Ising antiferromagnets with tricritical points, the meta model and the nnn model, and have studied their respective phase diagrams. The phase boundary in the H-T plane is mapped out, and estimates made for the location of the TCP's and the direct tricritical-susceptibility exponent $\bar{\gamma}$ in each model. The main results of the calculations are summarized in the phase diagrams of Fig. 7 of Paper I and Fig. 4 of II, and in the predictions for $\bar{\gamma}$ of Eq. (5.2) of I and Eq. (3.2) of II. Further, the series evidence supports the validity of the smoothness-postulate prediction of a constant exponent $\gamma_{st} = \frac{5}{4}$ for a wide range of fields along the second-order phase-transition line in both models.

Scaling at the TCP is discussed, especially double-power laws predicted to hold in the crossover region near the TCP. Our values for $\bar{\gamma}$ yield values for the TCP scaling power $\bar{a}_2$ ("weak"-direction scaling power) for each model. However, the inherent uncertainties in the series analysis and the spinodal continuation of the critical line make other scaling powers difficult to predict (assuming scaling indeed holds). A reliable determination of the crossover exponent φ is impossible to make. The behavior of the amplitudes for $\bar{\chi}_{st}$ allowed us to conclude only that the tricritical-staggered-susceptibility exponent $\bar{\gamma}_{st}$ is less than γ_{st} for the meta model, and about equal to γ_{st} for the nnn model.

The question of whether TCP scaling is obeyed in these two models still is open. The recent Monte Carlo results[16] for $\bar{\beta}$ would seem to cast not inconsiderable doubt upon at least a strong tricritical-scaling hypothesis applicable to both the first- and second-order lines. Series work on the BEG model produces results which may be inconsistent with TCP scaling.[17,18]

In conclusion, we note with interest and curiosity that these two models definitely show significant differences in behavior, the most striking being the different values for $\bar{\gamma}$. The amplitude behavior of $\bar{\chi}_{st}$ also is markedly different, and the spinodal hook goes up in the meta model, whereas it goes down for the nnn model. From universality arguments, one might expect that these models should behave similarly, since they are both three-dimensional Ising models. We do not know the answer to this puzzle, but can only speculate that there are several different kinds of TCP's in nature, both in models and probably in real materials as well. Further studies on TCP's, both model calculations and measurements on TCP properties of metamagnetic materials, would be very useful in elucidating some of these questions. Series work in conjunction with Monte Carlo work on the same TCP models seems to be a fruitful combination, especially if longer series and Monte Carlo calculations on bigger lattices become available. Looking further into the future, perhaps it will become possible to devise and study microscopic Hamiltonians whose critical behavior more closely simulates that in particular metamagnets when more experimental tricritical data becomes available, or even more complex systems (with, e.g., spin-flop transitions).

ACKNOWLEDGMENTS

The authors are indebted to Professor D. P. Landau, Professor R. B. Griffiths, Professor M. Wortis, and Professor T. S. Chang for invaluable correspondence and conversations concerning various aspects of this work. They are also very grateful for numerous discussions with R. Ditzian, A. Hankey, D. Karo, R. Krasnow, D. Lambeth, M. H. Lee, L. Liu, G. Paul, and D. Stauffer.

---

*Work forms portion of a Ph.D. thesis to be submitted to the Physics Department of MIT by F. H. Work supported by National Science Foundation, Office of Naval Research, and Air Force Office of Scientific Research. A preliminary report of portions of the present work appears in F. Harbus and H. E. Stanley, Phys. Rev. Lett. 29, 58 (1972).

†NSF Predoctoral Fellow.

[1]F. Harbus and H. E. Stanley, preceding paper, Phys. Rev. B 8, 1141 (1973) (hereafter referred to as I).

[2]R. B. Griffiths and J. C. Wheeler, Phys. Rev. A 2, 1047 (1970).

[3]J. Oitmaa, J. Phys. C 4, 2466 (1971); J. Phys. C 5, 435 (1972).

[4]D. P. Landau (private communication).

[5]D. P. Landau, Phys. Rev. Lett. 28, 449 (1972).

[6]E. K. Riedel, Phys. Rev. Lett. 28, 675 (1972).

[7]E. Riedel and R. Wegner, Z. Phys. 225, 195 (1969); Phys. Rev. Lett. 24, 730 (1970).

[8]A. Hankey, H. E. Stanley, and T. S. Chang, Phys. Rev. Lett. 29, 278 (1972); see also A. Hankey and H. E. Stanley, Phys. Rev. B 6, 3515 (1972); and T. S. Chang, A. Hankey and H. E. Stanley, Phys. Lett. A 44, 25 (1973).
[9]Throughout this general discussion of scaling, it is assumed that the phase boundary at the TCP is continuous, i.e., that the first- and second-order lines join smoothly. Further, we assume that the phase boundary in the physical plane (e.g., the H-T plane for antiferromagnets) is parallel to neither of the two in-plane axes at the TCP.
[10]Of course, in this affine field space, the notion of "orthogonality" really has no significance; any set of directions $(\bar{x}_1, \bar{x}_2, \bar{x}_3)$ at finite angles to each other would suffice.
[11]R. B. Griffiths, Phys. Rev. B 7, 545 (1973).
[12]That these paths are all equivalent is implicit in the geometrical concepts and viewpoint of Ref. 2.
[13]For a *detailed* derivation and treatment of double and other higher-order power laws, see T. S. Chang, A. Hankey, and H. E. Stanley, Phys. Rev. B 7, 4263 (1973); Phys. Rev. B 8, 346 (1973).
[14]F. Harbus and H. E. Stanley Phys. Rev. B (to be published). See also the work of P. Pfeuty, M. E. Fisher, and D. Jasnow on scaling predictions for crossover effects in anisotropic spir systems [AIP Conf. Proc. 10, 817 (1973)].
[15]L. Liu and H. E. Stanley, Phys. Rev. Lett. 29, 927 (1972); Phys. Rev. B (to be published).
[16]B. L. Arora and D. P. Landau, AIP Conf. Proc. (to be published).
[17]D. M. Saul and M. Wortis, AIP Conf. Proc. 5, 349 (1972).
[18]D. Stauffer (private communication).

PHYSICAL REVIEW B VOLUME 8, NUMBER 3 1 AUGUST 1973

Critical-Algebra Coefficients for the Three-Dimensional Ising Model*

R. Rutherford, III and Michael Wortis
Physics Department, University of Illinois, Urbana, Illinois 61801
(Received 26 March 1973)

High-temperature series expansions are used to test the reduction hypothesis of Kadanoff's operator algebra for the three-dimensional fcc Ising model with spin $s = 3/2, 2, \infty$. Agreement with our data is convincing. Numerical values are given for the coupling coefficients between the order parameter μ and μ^3 and between between μ^2 and the local energy density.

I. INTRODUCTION

In 1969 Kadanoff[1] proposed an "operator algebra" for thermodynamic critical fluctuations near second-order phase transitions.[2] According to this hypothesis there are in the critical region only a *finite* number of essentially different local operators $\mathcal{O}_\alpha(\vec{r})$, $\alpha = 1, 2, \ldots$, having divergent critical fluctuations. With each such fundamental critical operator is associated a critical index ω_α (now called the anomalous dimension of $\mathcal{O}_\alpha$[3]) such that

$$\langle \mathcal{O}_\alpha \rangle \sim B_\alpha t^{\nu(\omega_\alpha - \omega^*)} \tag{1}$$

and

$$\langle \mathcal{O}_\alpha(\vec{r})\, \mathcal{O}_\beta(\vec{0}) \rangle - \langle \mathcal{O}_\alpha \rangle \langle \mathcal{O}_\beta \rangle \sim \frac{D_{\alpha\beta}(t^\nu r)}{r^{\omega_\alpha + \omega_\beta - \omega^*}} , \tag{2}$$

where $0 < t = (T - T_c)/T_c \ll 1$, $r \gg a$ (lattice spacing), and external fields are set to zero. The amplitude B_α is constant in the critical region; $D_{\alpha\beta}(x)$ is a scaling function[2]; ν is the correlation length index. ω^*, the anomalous dimension of the vacuum, vanishes if two-exponent scaling[2] holds. The "reduction hypothesis"[1,4] then states that any local operator $Q(\vec{r})$ can be expressed near the critical point as the linear combination

$$Q(\vec{r}) \sim \sum_\alpha \Lambda_{Q\alpha} \mathcal{O}_\alpha(\vec{r}) + \text{nonsingular parts}, \tag{3}$$

and in particular for a nearby product of two fundamental operators

$$\mathcal{O}_\alpha(\vec{r})\, \mathcal{O}_\beta(\vec{r}') = \sum_\gamma \Lambda_{\alpha\beta,\gamma}(\vec{r} - \vec{r}') \mathcal{O}_\gamma[\tfrac{1}{2}(\vec{r} + \vec{r}')] + \text{nonsingular parts}, \tag{4}$$

provided $|\vec{r} - \vec{r}'| \ll \xi(t) \sim \xi_0 t^{-\nu}$ (the coherence length).

Kadanoff and Ceva[5] succeeded in constructing explicitly the critical algebra for the two-dimensional Ising model in zero field, and Kadanoff[1] showed how a knowledge of which coupling coefficients $\Lambda_{\alpha\beta,\gamma}$ are nonvanishing may serve to determine the critical exponents, thus deriving for the first time correct critical behavior by a method other than exact solution. Direct construction of the operator algebra has not so far been feasible for any other system; however, the recent renormalization group work initiated by Wilson[6] now provides a systematic framework in terms of which the relevant critical operators can be identified and the coupling coefficients (structure constants) Λ can in principle be evaluated.

Numerical tests of (3) and (4) have not been reported in the literature and the coupling coefficients are not in general known. It is the purpose of this paper to test the reduction hypothesis in the context of the three-dimensional face-centered-cubic spin-s Ising model in zero magnetic field by the use of the high-temperature series expan-